Quaternary Science Reviews 34 (2012) 57–65

Contents lists available at SciVerse ScienceDirect

Quaternary Science Reviews

journal homepage: www.elsevier.com/locate/quascirev

Stepwise expansions of C_4 biomass and enhanced seasonal precipitation and regional aridity during the Quaternary on the southern Chinese Loess Plateau

Jimin Sun [a,*], Tongyan Lü [a], Zhenqing Zhang [b], Xu Wang [a], Weiguo Liu [c]

[a] Key Laboratory of Cenozoic Geology and Environment, Institute of Geology and Geophysics, Chinese Academy of Sciences, P. O. Box 9825, Beijing 100029, China
[b] Northeast Institute of Geography and Agroecology, Chinese Academy of Sciences, Changchun 130012, China
[c] Institute of Earth Environment, Chinese Academy of Sciences, Xi'an 710075, China

ARTICLE INFO

Article history:
Received 16 February 2011
Received in revised form
28 November 2011
Accepted 8 December 2011
Available online 24 December 2011

Keywords:
Organic matter carbon isotope
Carbonate isotope
Aeolian deposits
Quaternary
Paleovegetation

ABSTRACT

The expansion of C_4 plants is one of the most prominent vegetation changes in the global ecosystem during the Cenozoic Era. Although C_4 plant expansions in the latest Miocene have been widely reported, factors driving the expansions are still in debate, and the details of vegetation changes during the Quaternary have not been well studied. Here we present high-resolution carbon isotope time series of both organic matter and bulk carbonates, covering the past 2.58 Ma, derived from the loess–soil successions on the southern Chinese Loess Plateau. The organic matter $\delta^{13}C$ values indicate stepwise C_4 plant expansions initiated at ~1.6 and at ~0.43 Ma, respectively. We conclude that such tectonic time scale C_4 plant expansions are controlled by enhanced seasonality of precipitation (relatively more precipitation in the warm growing season) as well as regional aridity, and this long-term fluctuation superimposes on the orbital scale variations of C_4 plants, while the latter appears phase-locked with cyclical changes of summer monsoon circulations.

1. Introduction

The aeolian deposits in China are generally regarded as one of the best long-term terrestrial records (e.g., Liu, 1985; Ding et al., 1992; Guo et al., 2002; Sun et al., 2010; Qiang et al., 2011). During the past decades, magnetic susceptibility and particle size are among the most commonly used parameters in reconstructing past climatic changes from aeolian deposits (e.g., Heller and Liu, 1982, 1984; An et al., 1991; Ding et al., 1994). Different from these physical proxies, the stable carbon isotope has been demonstrated to be an ideal tool in understanding terrestrial ecosystem on the Loess Plateau (e.g., Lin et al., 1991; Wang et al., 1997; Ding and Yang, 2000; Gu et al., 2003; Zhang et al., 2003; Vidic and Montañez, 2004; An et al., 2005; Liu et al., 2005a,b, 2011; Kaakinen et al., 2006; Ning et al., 2008; Passey et al., 2009; Yao et al., 2011).

The fractionation of carbon isotopes due to C_3 and C_4 photosynthetic mechanisms has been well documented (O'Leary, 1988; Farquhar et al., 1989). Both organic matter carbon isotope and soil pedogenic carbonate isotope have been used to estimate ecosystem changes. The C_3 plants have a mean $\delta^{13}C$ value of $-27‰$, whereas C_4 plants have a mean value of $-13‰$ (Deines, 1980; Farquhar et al., 1989). Soil organic matter preserves this isotope distinction with little or no fractionation (Melillo et al., 1989; Cerling et al., 1997). Therefore, the $\delta^{13}C$ values of soil organic matter can be used to estimate past C_3/C_4 ratios. Different from the organic matter carbon isotope, the formation of the soil carbonate is partially related to the pCO_2 level of soil solution, which is associated with plant respired CO_2 (Cerling, 1991, 1999). In this sense, the isotope values of pedogenic carbonate can be used to reconstruct paleoecological changes (Amundson et al., 1989; Quade et al., 1989; Kelly et al., 1991). In general, the carbon isotopic composition of pedogenic carbonate is related to the C_3/C_4 vegetation present in soil (Cerling, 1984). Based on this principle, expansion of C_4 plants during late Miocene was demonstrated by studying carbonate isotopes (Quade et al., 1989; Cerling et al., 1997; Pagani et al., 1999).

Recently, long-term C_3/C_4 evolution history on the Chinese Loess Plateau has also been studied (e.g., Ding and Yang, 2000; Jiang et al., 2002; An et al., 2005; Kaakinen et al., 2006; Passey et al., 2009). Based on the $\delta^{13}C$ record of soil carbonate, Ding and Yang (2000) reported a major expansion of C_4 plants at ca 4.0 Ma in the middle Loess Plateau, similar result was reported by Jiang et al. (2002). In the northern Loess Plateau, recent study on soil carbon and tooth enamel isotopes demonstrates that the C_4 vegetation was present by late Miocene time (Passey et al., 2009). Different from the above results, another $\delta^{13}C$ record of soil carbonate from the southern Loess Plateau indicates that the C_4 component was negligible before

* Corresponding author. Tel.: +86 10 8299 8389.
E-mail address: jmsun@mail.igcas.ac.cn (J. Sun).

0277-3791/$ – see front matter © 2011 Elsevier Ltd. All rights reserved.
doi:10.1016/j.quascirev.2011.12.007

2.7 Ma (Kaakinen et al., 2006). Moreover, An et al. (2005) reported two high-resolution carbon isotope time series, covering the past 7 Ma, and indicated that three intervals of significant C_4 plant expansions within the semiarid monsoonal region of East Asia (ca 2.9–2.7 Ma, 1.3–0.9 Ma, and 0.6 Ma–present). Obviously, different opinions do exist about long-term C_4 plant expansions on the Loess Plateau.

In this paper, we construct high-resolution carbon isotopic records covering the whole Quaternary in order to address two questions: (1) long-term vegetation changes on the southern Loess Plateau, and (2) factors driving the expansion of C_4 plants within the Quaternary.

2. Geological setting and stratigraphy

The studied Yanyu section (34°20′37″N, 109°31′14″E) is located in the southern Loess Plateau (Fig. 1a), with an elevation of approximately 620 m above sea level (Sun, 2005). This section belongs to the highest loess terrace in the northern piedmont of the west-east stretching Qinling Mountains (Fig. 1b), and this range is a biogeographic barrier between the temperate Loess Plateau to the north and sub-tropical southern China.

The climate of the southern Loess Plateau is controlled by the warm/humid east Asian monsoon in the summer season and the cold/dry northwest winds in the winter season (Fig. 2a). The studied Yanyu section has a mean annual precipitation of about 600 mm (Fig. 2a) and temperature of 13.2 °C (Fig. 2b).

The present vegetation on the loess terrace at Yanyu has been mostly destroyed by human cultivation, but herbs and shrubs dominated by *Vitex negundo* var. *heterophylla*, *Zizyphus jujuba* var. *spinosa*, and *Bothriochloa ischaemum* grow in slopes of loess valleys (Sun et al., 1995). Organic matter carbon isotope data of modern surface soil suggests that the current vegetation is a mixture of C_3 and C_4 plants, but dominated by C_3 plants (Liu et al., 2011).

The aeolian deposits at Yanyu have a thickness of 157.7 m (Fig. 3). The loess–soil successions can be subdivided into 33 loess beds (from L1 to L33, L represents loess) and 33 paleosols (S0 to S32, S represents soil).

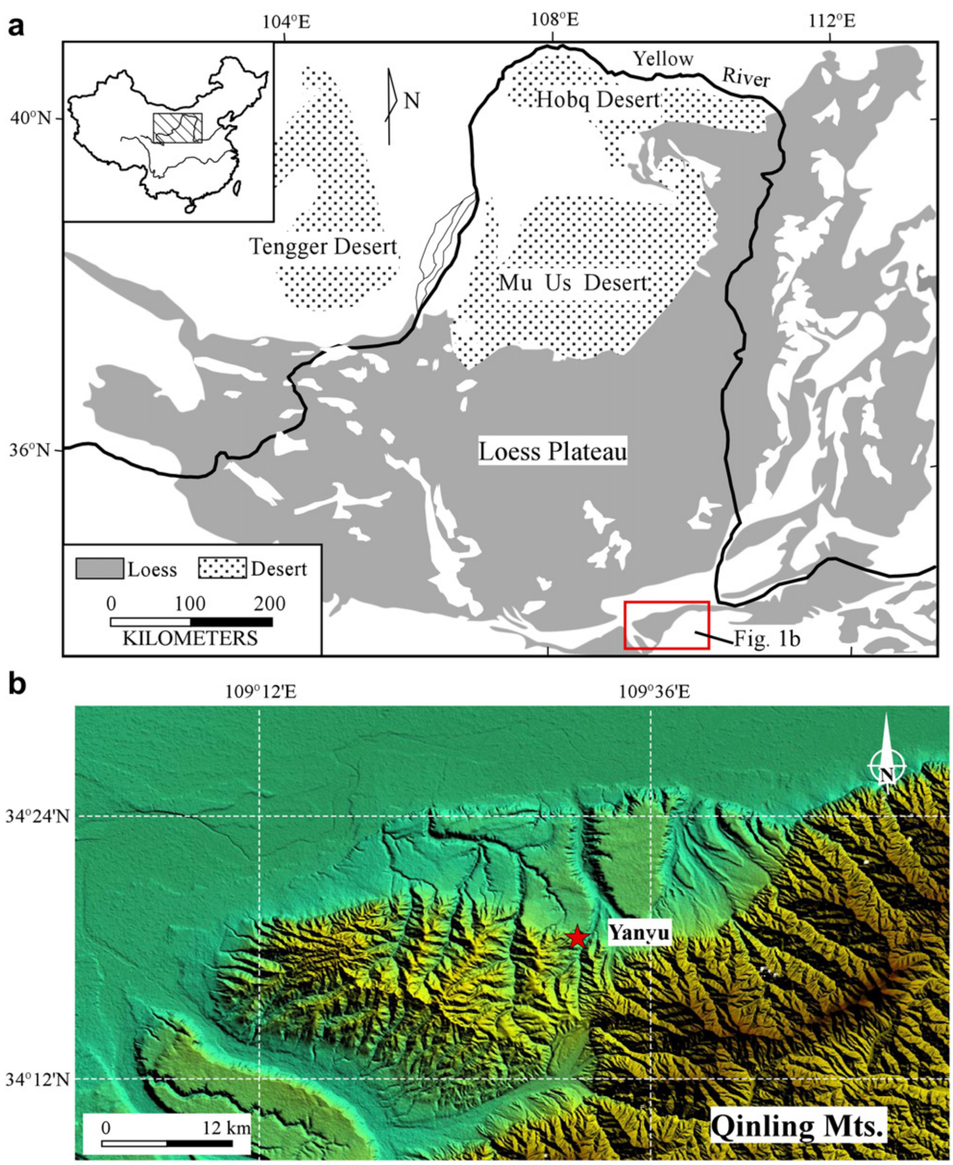

Fig. 1. Maps show the loess distributions on the Chinese Loess Plateau (a) and the Digital Elevation Model (DEM) image (data from the 90 m resolution DEM database) of the studied region (b).

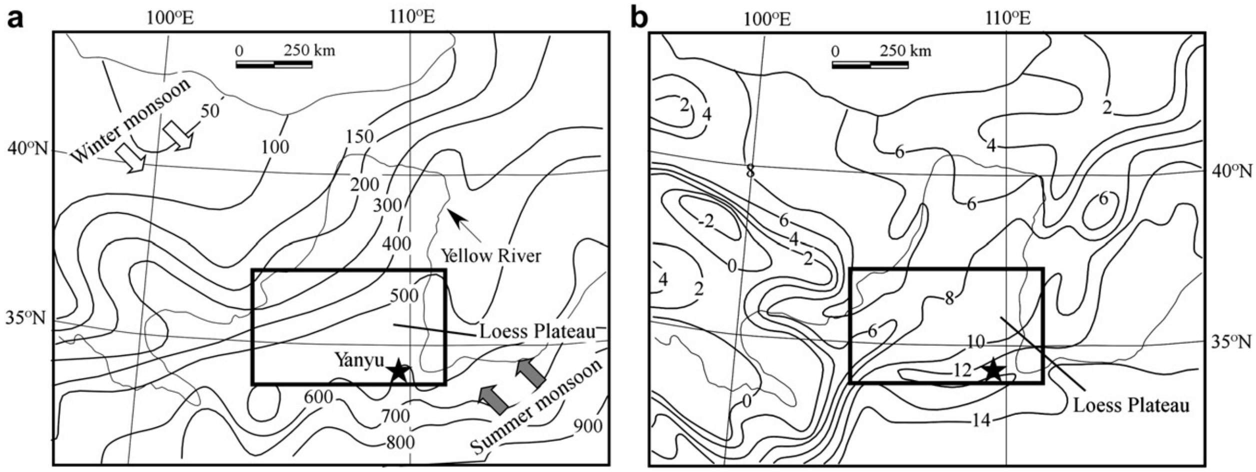

Fig. 2. Maps show the mean annual precipitation (a) and temperature (b) in north China (after Zhao, 1995). The rectangle box indicates the location of the Loess Plateau. Noting the zonal decrease trends of both precipitation and temperature due to the northwestly weakened summer monsoon.

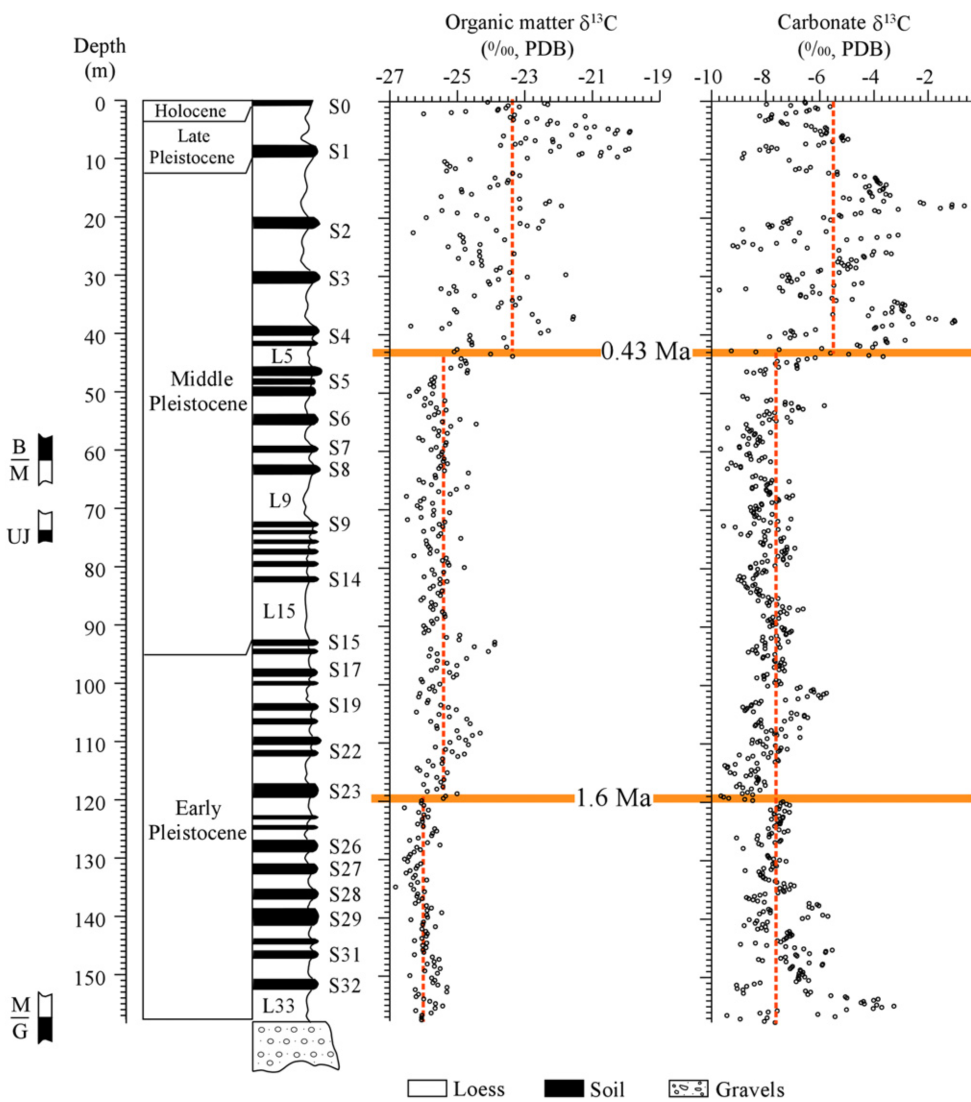

Fig. 3. The $\delta^{13}C$ records of both organic matter and bulk carbonates during the Quaternary. The bold orange lines indicating the stepwise increase of organic matter carbon isotopes occurring at ca 1.6 Ma and ca 0.43 Ma. For the $\delta^{13}C$ record of bulk carbonates, only the increase of $\delta^{13}C$ values after 0.43 Ma is significant. The B/M boundary and Upper Jaramillo (UJ) normal subchron are after Zhu et al. (1994), and M/G boundary is from Ding et al. (1991). (For interpretation of the references to color in this figure legend, the reader is referred to the web version of this article.)

Chronology of Chinese loess has been well established mainly by using a combination of approaches of magnetostratigraphy and climatostratigraphy (e.g., Heller and Liu, 1982, 1984; Liu, 1985; Kukla, 1987). Previous palaeomagnetic polarity studies at Yanyu were completed by Ding et al. (1991) and Zhu et al. (1994). The Matuyama/Gauss (M/G) boundary was found in the lower part of L33 (Ding et al., 1991), while the Brunhes/Matuyama (B/M) boundary and the Upper Jaramillo (UJ) subchron were found in L8 and in the units from L10 to S11, respectively (Zhu et al., 1994, Fig. 3). The above chronology demonstrates that the Quaternary aeolian deposits at Yanyu have a basal age of 2.58 Ma.

3. Material and methods

In this study, 418 samples for organic matter carbon isotope analysis were taken with two different sampling intervals: fifty samples were taken above the Last Interglacial soil (S1) with a sampling interval of 20 cm; all the other samples (below S1) were taken with a sampling interval of 30 cm. Moreover, 788 bulk samples for carbonate carbon isotope analysis were taken with 20 cm sampling interval. Samples for magnetic susceptibility analysis above S1 were taken with 10 cm sampling interval.

Samples for organic matter carbon stable isotope analysis were first screened for modern rootlets and then digested for at least 15 h in 1 M HCl to remove inorganic carbonate. The samples were then washed with distilled water and dried. The dried samples (~480 mg) were combusted for over 4 h at 900 °C in evacuated sealed quartz tubes in the presence of 0.5 g Cu, 4.5 g CuO and 0.2 g Ag foil. The CO_2 was purified and isolated by cryogenic distillation for isotopic analysis. The isotopic composition of CO_2 was then measured using a Finnigan MAT 253 mass spectrometer and reported in per mil units (x) relative to Vienna Peedee belemnite (V-PDB) standard. Recurrent analyses ($n = 9$) show that this procedure yields a precision better than ±0.2‰.

Bulk samples for carbonate carbon isotope analysis were ground to powder, and converted to CO_2 with 100% phosphoric acid. Carbon isotopic measurements were made in the Environmental Isotope Laboratory of the Institute of Geology and Geophysics, Chinese Academy of Science, using a MAT−253 mass spectrometer linked to a Gas Bench−II (Thermo−Finnigan). The precision is 0.1‰ (1σ), and the precision were routinely checked by running the carbonate standard NBS-19 after every six sample measurements. All isotope values are reported in parts per mil (‰) relative to V-PDB.

The magnetic susceptibility measurements were completed by using a Bartington M.S.2 magnetic susceptibility bridge. Mass (dry-weight based) magnetic susceptibility was measured in the laboratory.

The microstructure of the pedogenic carbonate from the last glacial loess bed was examined by scanning electron microscope (SEM), using a LEO 1450VP instrument with Oxford INCA energy microanalysis system at the Institute of Geology and Geophysics, Chinese Academy of Sciences.

4. Results

The $\delta^{13}C$ curves of the organic matter and bulk carbonate of the Yanyu section are shown in Fig. 3. The $\delta^{13}C$ values of the organic matter range from −26.8‰ to −19.9‰ with a mean value of −24.9‰; whereas the $\delta^{13}C$ values of carbonate varies from −9.7‰ to −0.7‰ with a mean value of −7.1‰. Examination of the long-term carbon isotope records indicates the following major properties.

Firstly, the general variation trend of $\delta^{13}C$ values of organic matter is characterized by stepwise increase occurred above the middle part of L5 and above the base of S23 (Fig. 3). According to the stacked 2.6-Ma time scale of the Chinese loess (Ding et al., 2002), the corresponding ages are 0.43 and 1.6 Ma, respectively (Fig. 3). The averaged $\delta^{13}C$ value of organic matter is −26‰ between 2.58 and 1.6 Ma, it increases to −25.5‰ between 1.6 and 0.43 Ma, and ultimately increases to −23.4‰ after 0.43 Ma (Fig. 3). Organic matter formed in the presence of a pure C_3 and C_4 biomass would have mean $\delta^{13}C$ values of ~−27‰ and −13‰, respectively (Deines, 1980; Farquhar et al., 1989). Our $\delta^{13}C$ record suggests that the vegetation of the southern Loess Plateau consists of both C_3 and C_4 plants during the last 2.58 Ma. The proportion of C_4/C_3 vegetation is estimated based on the average end member of pure C_3 and C_4

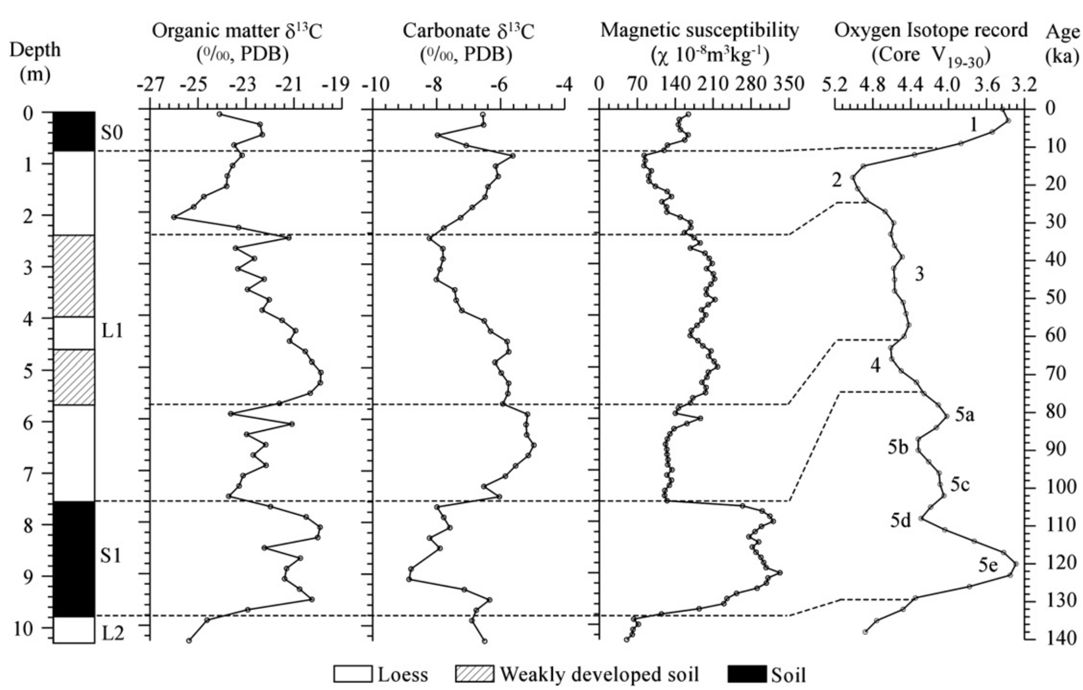

Fig. 4. Correlation between the $\delta^{13}C$ records of both organic matter and bulk carbonate and the low-frequency (470 Hz) mass magnetic susceptibility curve as well as the marine oxygen isotopic curve of V_{19-30} (Shackleton and Pisias, 1985) during the last glacial–interglacial cycle.

plants by using the method of Liu et al. (2003). The averaged C_4 plant proportions increased from 7.1%, prior to 1.6 Ma, to 10.7% between 1.6 and 0.43 Ma, and further increased to 25.7% after 0.43 Ma.

Secondly, Fig. 3 clearly indicates that there is a remarkable increase trend of carbonate carbon isotopes toward higher $\delta^{13}C$ values initiated ~0.43 Ma ago. The mean value of carbonate $\delta^{13}C$ increases from −7.7‰ prior to 0.43 Ma to −5.5‰ after 0.43 Ma. Because bulk sample carbonates contain both pedogenic and detrital origins, the $\delta^{13}C$ values of the bulk carbonate cannot be simply used to estimate C_4/C_3 proportions.

5. Discussions

5.1. Mechanism for carbon isotopic variations on glacial–interglacial cycles

In order to discuss the mechanism of carbon isotopic variations on orbital time scales, we compare the $\delta^{13}C$ records of both organic matter and bulk carbonate with the mass magnetic susceptibility curve and the marine oxygen isotopic time series of V_{19-30} (Shackleton and Pisias, 1985) during the last glacial–interglacial cycle (Fig. 4).

Firstly, the $\delta^{13}C$ record of organic matter is characterized by the higher $\delta^{13}C$ values in paleosols and the lower values in loess beds (Fig. 4), implying more C_4 plants during the Last Interglacial. This is consistent with previous results (e.g., Lin et al., 1991; Zhang et al., 2003; Liu et al., 2005a,b; Ning et al., 2008). The peak-trough fluctuations of $\delta^{13}C$ values of organic matter correlate well with the variations of the magnetic susceptibility curve, which has been used as a proxy of east Asian summer monsoon strength (e.g., An et al., 1991).

Because C_4 plants favor C_3 plants at times of higher temperature (e.g., Gu et al., 2003; Zhang et al., 2003) and/or summer precipitation (An et al., 2005; Liu et al., 2005b), the higher $\delta^{13}C$ values and thus higher proportion of C_4 plants during the Holocene and the last interglaciation can be generally attributed to the higher temperature and summer precipitation, which are ultimately controlled by summer monsoon strength.

Therefore, the good correlation between the $\delta^{13}C$ record of organic matter and the marine oxygen isotope curve demonstrates that the C_4/C_3 proportions of loess deposits are dominantly controlled by summer monsoon strength on orbital time scales (glacial–interglacial cycles). This explanation can be further supported by the decreasing trend of $\delta^{13}C$ values of modern surface soil organic matter from the southeast to the northwest Loess Plateau (Liu et al., 2011), mirrored by the same decreasing trend of the summer monsoon strength.

Except the variations on glacial–interglacial cycles, the last glacial loess of L1 at Yanyu can be further subdivided into five parts (Fig. 4). Two weakly developed soil beds can be easily distinguished within L1, this is the common pedostratigraphic property on the southern Loess Plateau (e.g., Guo et al., 1996; Sun et al., 2010). These two weak soils together with the interbedded loess bed,

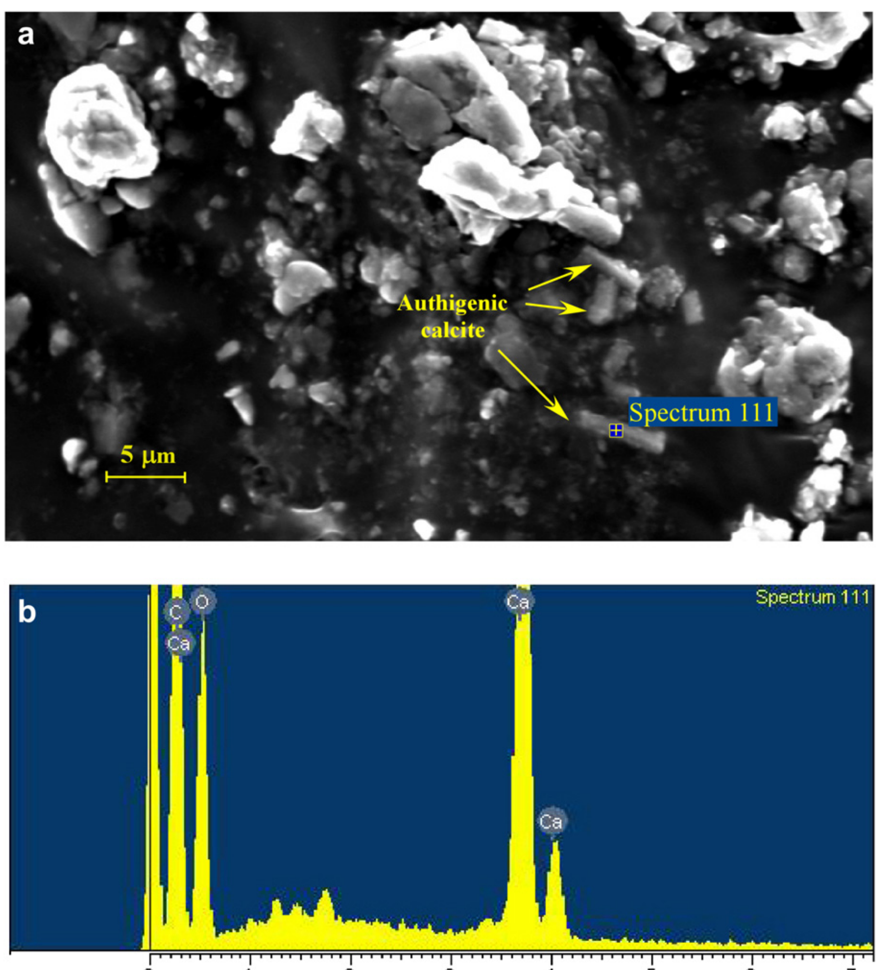

Fig. 5. Scanning electron microscopy images of the euhedral calcite crystals (pedogenic origin) of the last glacial loess at Yanyu (a) and the abundance of elements of the pedogenic calcite measured by the equipped energy microanalysis system (b).

corresponding to marine Oxygen Isotope Stage 3 (Fig. 4). These two weak soils are also characterized by the relatively higher $\delta^{13}C$ values of organic matter.

Secondly, contrary to the variations of $\delta^{13}C$ values of organic matter, the $\delta^{13}C$ record of bulk carbonate shows higher values in glacial loess beds (Fig. 4). Although pedogenic origin carbonates of the euhedral calcite crystals with lengths of 2–5 μm can be identified from the last glacial bed with the help of scanning electron microscopy technique (Fig. 5), the bulk carbonate is though to be a mixture of detrital carbonates and authigenic soil carbonates (e.g., Wen, 1989). Different from the pedogenic carbonate, the detrital carbonates are dominantly derived from paleo-marine sediments which have higher $\delta^{13}C$ values in the source regions (e.g., Liu et al., 2005b, 2011). Therefore, the $\delta^{13}C$ record of bulk carbonate cannot be directly used to estimate C_4 plant proportion (Liu et al., 2011), but it can be used to estimate the relative contribution of pedogenic carbonate. Therefore, the higher $\delta^{13}C$ values of bulk carbonate in loess bed can be explained as the influx of more detrital carbonates as well as the less formation of pedogenic carbonates due to the weakened strength of summer monsoon during glacial period. In this sense, the $\delta^{13}C$ variations of both organic matter and bulk carbonate can be explained by changed summer monsoon strength on orbital time scales on the Loess Plateau.

5.2. Factors driving stepwise C_4 plant expansions on tectonic time scales (on the levels of millions of years) on the southern Loess Plateau

The carbonate isotopic record of organic matter from the southern Loess Plateau indicates stepwise expansions of C_4 plants initiated at ~1.6 Ma and at ~0.43 Ma (Fig. 6). A question occurs: what factors account for the stepwise C_4 plant expansions during the Quaternary?

By now, there have been many different opinions about the long-term C_4 plant evolution. Quade et al. (1989) attributed the expansion of C_4 biomass in the latest Miocene to the inception or a marked strengthening of the Asian monsoon system. An et al. (2005) argued that the C_4 plant expansions on the Loess Plateau have been driven by east Asian summer monsoon circulation. Different from the above arguments, Cerling et al. (1993, 1997) suggested that the decrease of atmospheric CO_2 concentration is responsible for the C_4 biomass expansion. Huang et al. (2001) proposed that regional climate exerted a strong control on the relative abundance of C_3 and C_4 plants and low pCO_2 alone is insufficient to drive an expansion of C_4 plants. Another opinion attributed this ecological event to enhanced aridity (e.g., Pagani et al., 1999; Dettman et al., 2001).

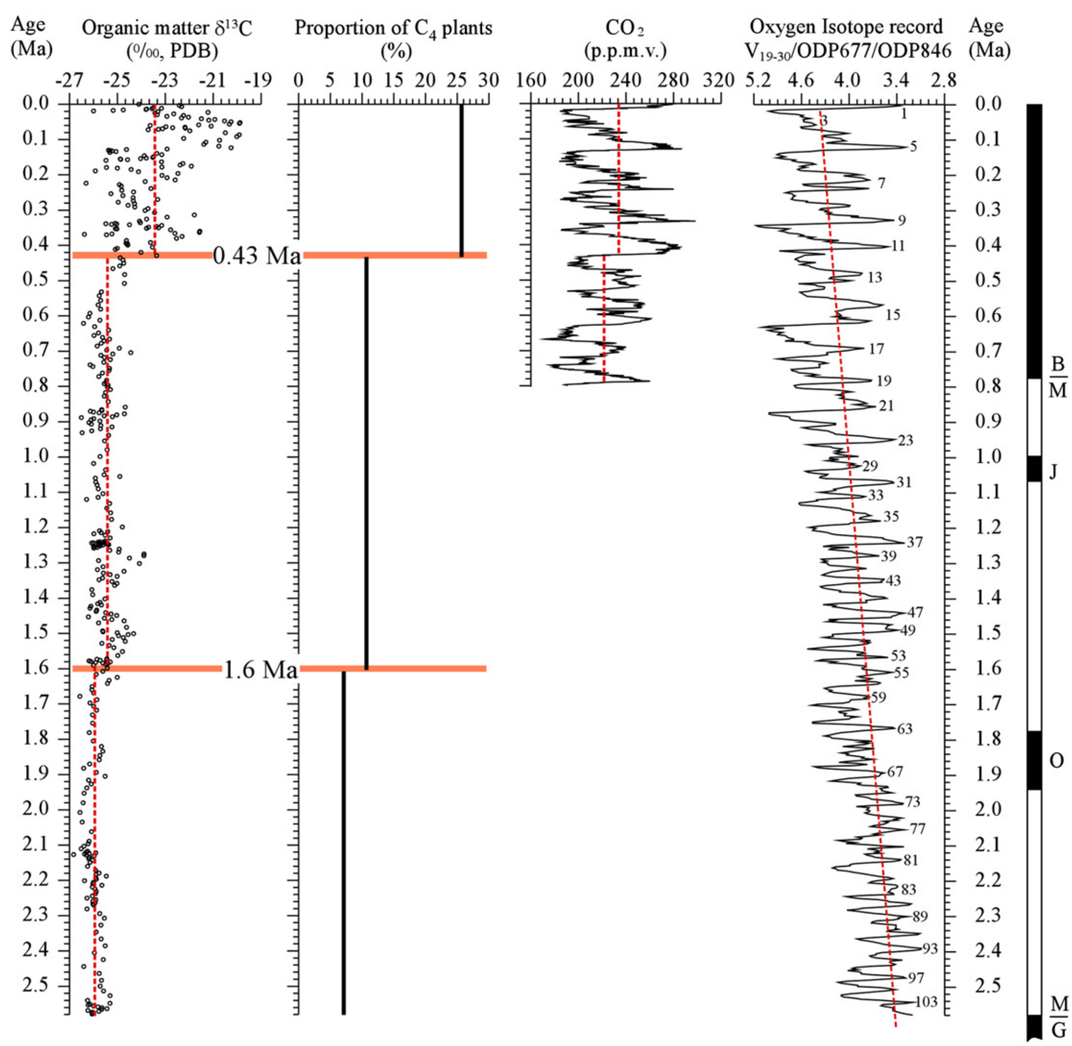

Fig. 6. The $\delta^{13}C$ curve of organic matter and the C_4 expansion events at Yanyu are compared with the atmospheric CO_2 concentrations of the past 0.8 Ma as well as the composite marine oxygen isotope record. The CO_2 data are from Lüthi et al. (2008). The isotope curve is a composite record of V_{19-30} (0–0.34 Ma, Shackleton and Pisias, 1985), ODP 677 (0.34–1.811 Ma, Shackleton et al., 1990) and ODP 846 (1.811–2.58 Ma, Shackleton et al., 1995a,b).

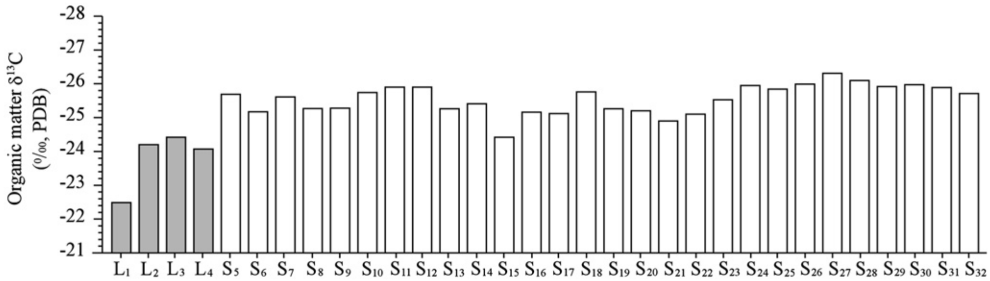

Fig. 7. Correlation between the organic matter $\delta^{13}C$ values of four loess beds (L_1–L_4) and that of the paleosols (from S5 to S32) at Yanyu.

In this study, in order to explore the mechanism of the stepwise expansions of C_4 plants on tectonic time scale, we compare the $\delta^{13}C$ curve of organic matter and the C_4 expansion events at Yanyu with the atmospheric CO_2 concentrations of the past 0.8 Ma as well as the composite marine oxygen isotope record during the Quaternary (Fig. 6). The age control for the Yanyu section is tuned based on the stacked 2.6 Ma time scale of the Chinese loess (Ding et al., 2002).

For the long-term vegetation changes, Cerling et al. (1993) proposed that C_4 plant expansion in the late Miocene was associated with a significant reduction of atmospheric pCO_2 levels. However, our results indicate that generally higher $\delta^{13}C$ values and thus more C_4 plants occur in interglaciations (Figs. 4 and 6), corresponding to higher pCO_2 levels (Fig. 6). This does not support a dominant pCO_2 control on the observed $\delta^{13}C$ variations within the Quaternary. Moreover, when we examine in detail, it is easily to find that the mean value of the atmospheric CO_2 concentrations is higher after 0.43 Ma. If the low atmospheric CO_2 concentration is the sole factor controlling the C_4 biomass expansion as suggested by Cerling et al. (1993, 1997), we should find a decrease trend of $\delta^{13}C$ values after 0.43 Ma. Obviously, this is contrary to our observations. Therefore, although the decrease of atmospheric CO_2 concentration may be important for the origin and early expansions of C_4 plants in the Tertiary (e.g., Pearcy and Ehleringer, 1984), the low pCO_2 alone is not sufficient to drive an expansion of C_4 plants during the Quaternary.

Although the C_4 plant variations on orbital time scales are attributed to the relatively intensified summer monsoon, the observed stepwise expansions on tectonic time scale cannot be explained by strengthened summer monsoon. We have two lines of evidence. Firstly, the long-term variations of marine oxygen isotopes suggest increasing ice volume from the beginning of the Quaternary to present (Fig. 6), the enlarging ice sheet in the high latitude of the northern Hemisphere favored cold air outbreaks and then the much enhanced winter monsoon. Moreover, the gradually lowering global sea level (decreased ocean/land ratio), together with the less surface water evaporation (due to the low sea surface temperature in tropical and sub-tropical oceans), led to the generally long-term weakened summer monsoon. Therefore, the stepwise expansions of C_4 plants initiated at ~1.6 Ma and at ~0.43 Ma cannot be interpreted by enhanced east Asian summer monsoon. Secondly, we compare the organic matter $\delta^{13}C$ values of four loess beds (L_1–L_4) with that of the paleosols (from S5 to S32) which indicate that the $\delta^{13}C$ values of the above glacial loess beds are higher (more C_4 plants) than the subsequent interglacial soils (Fig. 7). By now, there has no evidence to demonstrate that the summer monsoon winds in glacial periods were stronger than in interglacial episodes. Therefore, the above evidence also supports that the long-term variation trend of C_4 plants are not simply controlled by summer monsoon strength.

We propose that two factors can account for the stepwise expansions of C_4 plants in the southern Loess Plateau. Firstly, summer rainfall in growing season can promote expansion of C_4 grasses in the arid and semiarid regions (Connin et al., 1998). Although the long-term variation trend of the summer monsoon strength generally decreased from the beginning of the Quaternary to present, implying decreasing annual precipitation, the seasonal distributions of the precipitation changed during the Quaternary. The observed long-term stepwise expansions of C_4 plants can be related to the much enhanced seasonality of the precipitation. It means more summer rainfall in growing season (favors C_4 plant growing) and less precipitation in the winter season. Therefore, the expansions of C_4 plants initiated at 1.6 Ma and 0.43 Ma can be dominantly controlled by the stepwise enhanced seasonal precipitation. Our results suggest that there exists a trend of toward more summer rainfall on the southern Loess Plateau, and this is especially more striking since the Mid-Brunhes Event of 0.43 Ma ago.

Secondly, it is also generally agreed that C_4 plants have greater water-use efficiency than C_3 plants (Raven et al., 1999). Thus, modern C_4 plants are commonly distributed in hot and dry environments in tropical and sub-tropical regions (Cerling et al., 1997). The larger-scale tendency toward global cooling and weakened summer monsoon since the beginning of the Quaternary imply long-term aridity trend. Therefore, the stepwise enhanced regional aridity plays another role in controlling the long-term C_4 plant expansions on the southern Loess Plateau. According to our interpretation, the most significant C_4 plant expansion and then the much enhanced aridity initiated at ~0.43 Ma ago (Fig. 6). This can be supported by the increases of aeolian flux in the North Pacific Ocean (Hovan et al., 1991) and a major change to 'fully arid conditions' at about 0.5 Ma ago in Australia (Martin, 2006).

6. Conclusions

High-resolution $\delta^{13}C$ records of both organic matter and bulk carbonates are reconstructed from the southern Loess Plateau during the Quaternary. Different from the $\delta^{13}C$ values of bulk carbonates, which are controlled by both detrital and pedogenic carbonates, the organic matter carbon isotopes can be used to estimate paleovegetations. Higher organic matter $\delta^{13}C$ values and thus more C_4 plants occur in interglacial times, whereas lower $\delta^{13}C$ values and less C_4 biomass occur in glacial stages. The variations of organic matter $\delta^{13}C$ values are mainly controlled by summer monsoon strength on orbital time scales. However, the long-term variation trend of the $\delta^{13}C$ values cannot be simply explained by the summer monsoon strength. We propose that the stepwise expansions of C_4 plants initiated at ca 1.6 and ca 0.43 Ma are controlled by enhanced seasonality of precipitation (relatively more precipitation in the warm growing season) as well as regional aridity. The orbital scale variations of C_4 plants driven by summer monsoon circulation superimpose on the long-term trend of tectonic time scales.

Acknowledgments

This work was supported by the National Nature Science Foundation of China (Grant 40830104), the National Basic Research

Program of China (2010CB833400), and the Chinese Academy of Sciences (KZCX2-YW-Q09-06-04). We thank the two anonymous reviewers for their very helpful comments.

References

Amundson, R.G., Chadwick, O.A., Sowers, J.M., Doner, H.E., 1989. The stable isotope chemistry of pedogenic carbonates at Kyle Canyon, Nevada. Soil Science Society of America Journal 53, 201–210.

An, Z.S., Huang, Y.S., Liu, W.G., Guo, Z.T., Clemens, S., Li, L., Prell, W., Ning, Y.F., Cai, Y.J., Zhou, W.J., Lin, B.H., Zhang, Q.L., Cao, Y.N., Qiang, X.K., Chang, H., Wu, Z.K., 2005. Multiple expansions of C_4 plant biomass in East Asia since 7 Ma coupled with strengthened monsoon circulation. Geology 33, 705–708.

An, Z.S., Kukla, G., Porter, S.C., Xiao, J.L., 1991. Magnetic susceptibility evidence of monsoon variation on the Loess Plateau of Central China during the last 130,000 years. Quaternary Research 36, 29–36.

Cerling, T.E., 1984. The stable isotopic composition of modern soil carbonate and its relationship to climate. Earth and Planetary Science Letters 71, 229–240.

Cerling, T.E., 1991. Carbon dioxide in the atmosphere: evidence from Cenozoic and Mesozoic paleosols. American Journal of Science 291, 377–400.

Cerling, T.E., 1999. Stable carbon isotopes in palaeosol carbonates. Special Publication of the International Association of Sedimentologists 27, 43–60.

Cerling, T.E., Harris, B., MacFadden, M., Leakey, J., Quade, V., Elsenmann, J., Ehleringer, J.R., 1997. Global vegetation change through the Miocene/Pliocene boundary. Nature 389, 153–158.

Cerling, T.E., Wang, Y., Quade, J., 1993. Expansion of C_4 ecosystems as an indicator of global ecological change in the late Miocene. Nature 361, 344–345.

Connin, S.L., Betancourt, J., Quade, J., 1998. Late Pleistocene C_4 plant dominance and summer rainfall in the southwestern United States from isotopic study of herbivore teeth. Quaternary Research 50, 179–193.

Deines, P., 1980. The isotopic composition of reduced organic carbon. In: Firtz, P., Fontes, J.Ch. (Eds.), Handbook of Environmental Isotope Geochemistry. Elsevier, New York, pp. 331–406.

Dettman, D.L., Kohn, M.J., Quade, J., Ryerson, F.J., Ojha, T.P., Hamidullah, S., 2001. Seasonal stable isotope evidence for a strong Asian monsoon throughout the past 10.7 m.y. Geology 29, 31–34.

Ding, Z.L., Derbyshire, E., Yang, S.L., Yu, Z.W., Xiong, S.F., Liu, T.S., 2002. Stacked 2.6-Ma grain size record from the Chinese loess based on five sections and correlation with the deep-sea $\delta^{18}O$ record. Paleoceanography 17, 1033. doi:10.1029/2001PA000725.

Ding, Z.L., Rutter, N., Han, J.T., Liu, T.S., 1992. A coupled environmental system formed at about 2.5 Ma in East Asia. Palaeogeography, Palaeoclimatology, Palaeoecology 94, 223–242.

Ding, Z.L., Rutter, N., Liu, T.S., Evans, M.E., Wang, Y.C., 1991. Climatic correlation between Chinese loess and deep-sea cores: a structural approach. In: Liu, T.S. (Ed.), Loess, Environment and Global Change. Science Press, Beijing, pp. 168–186.

Ding, Z.L., Yang, S.L., 2000. C_3/C_4 vegetation evolution over the last 7.0 Myr in the Chinese Loess Plateau: evidence from pedogenic carbonate $\delta^{13}C$. Palaeogeography, Palaeoclimatology, Palaeoecology 160, 291–299.

Ding, Z.L., Yu, Z.Y., Rutter, N.W., Liu, T.S., 1994. Towards an orbital time scale for Chinese loess deposits. Quaternary Science Reviews 13, 39–70.

Farquhar, G., Ehleringer, J., Hubick, K., 1989. Carbon isotope discrimination and photosynthesis. Annual Review of Plant Physiology 40, 503–537.

Gu, Z.Y., Liu, Q., Xu, B., Han, J.M., Yang, S.L., Ding, Z.L., Liu, T.S., 2003. Climate as the dominant control on C_3 and C_4 plant abundance in the Loess Plateau: evidence of organic carbon isotope records from the last glacial–interglacial loess–paleosol sequences. Chinese Science Bulletin 48, 1271–1276.

Guo, Z., Liu, T., Guiot, J., Wu, N., Lü, H., Han, J., Liu, J., Gu, Z., 1996. High frequency pulses of East Asian monsoon climate in the last two glaciations: link with the North Atlantic. Climate Dynamics 10, 701–709.

Guo, Z.T., Ruddiman, W.F., Hao, Q.Z., Wu, H.B., Qiao, Y.S., Zhu, R.X., Peng, S.Z., Wei, J.J., Yuan, B.Y., Liu, T.S., 2002. Onset of Asian desertification by 22 Myr ago inferred from loess deposits in China. Nature 416, 159–163.

Heller, F., Liu, T.S., 1982. Magnetostratigraphic dating of loess deposits in China. Nature 300, 431–433.

Heller, F., Liu, T.S., 1984. Magnetism of Chinese loess deposits. Geophysical Journal of the Royal Astronomical Society 77, 125–141.

Hovan, S.A., Rea, D.K., Pisias, N.G., 1991. Late Pleistocene continental climate and oceanic variability recorded in Northwest Pacific sediments. Paleoceanography 6, 349–370.

Huang, Y., Street-Perrott, F.A., Metcalfe, S.E., Brenner, M., Moreland, M., Freeman, K.H., 2001. Climate change as the dominant control on glacial–interglacial variations in C_3 and C_4 plant abundance. Science 293, 1647–1651.

Jiang, W.Y., Peng, S.Z., Hao, Q.Z., Liu, T.S., 2002. Carbon isotopic records in paleosols over the Pliocene in Northern China: implication on vegetation development and Tibetan uplift. Chinese Science Bulletin 47, 687–690.

Kaakinen, A., Sonninen, E., Lunkka, J.P., 2006. Stable isotope record in paleosol carbonates from the Chinese Loess Plateau: implications for late Neogene paleoclimate and paleovegetation. Palaeogeography, Palaeoclimatology, Palaeoecology 237, 359–369.

Kelly, E.F., Amundson, R.F., Marino, B.D., DeNiro, M.J., 1991. Stable carbon isotopic composition of carbonate in Holocene grassland soils. Soil Science of America Journal 55, 1651–1658.

Kukla, G., 1987. Loess stratigraphy in central China. Quaternary Science Reviews 6, 191–219.

Lin, B.H., Liu, R.M., An, Z.S., 1991. Preliminary research on stable isotopic compositions of Chinese loess. In: Liu, T.S. (Ed.), Loess, Environment and Global Change. Science Press, Beijing, pp. 124–131 (in Chinese).

Liu, L., Zhou, X., Yu, Y.Y., Guo, Z.T., 2011. The natural vegetations on the Chinese Loess Plateau: the evidence of soil organic carbon isotope. Quaternary Sciences 31, 506–513 (in Chinese).

Liu, T.S., 1985. Loess and the Environment. China Ocean Press, Beijing, 251 pp.

Liu, W., An, Z., Zhou, W., Heada, M.J., Cai, D., 2003. Carbon isotope and C/N ratios of suspended matter in rivers – An indicator of seasonal change in C_4/C_3 vegetation. Applied Geochemistry 18, 1241–1249.

Liu, W.G., Feng, X.H., Ning, Y.F., Zhang, Q.L., Cao, Y.N., An, Z.S., 2005a. $\delta^{13}C$ variation of C_3 and C_4 plants across an Asian monsoon rainfall gradient in arid northwestern China. Global Change Biology 11, 1094–1100.

Liu, W.G., Huang, Y.S., An, Z.S., Clemens, S.C., Li, L., Prell, W.L., Ning, Y.F., 2005b. Summer monsoon intensity controls C_4/C_3 plant abundance during the last 35 ka in the Chinese Loess Plateau: carbon isotope evidence from bulk organic matter and individual leaf waxes. Palaeogeography, Palaeoclimatology, Palaeoecology 220, 243–254.

Liu, W.G., Yang, H., Sun, Y.B., Wang, X.L., 2011. $\delta^{13}C$ values of loess total carbonate: a sensitive proxy for Asian summer monsoon in arid northwestern margin of the Chinese loess plateau. Chemical Geology 284, 317–322.

Lüthi, D., Le Floch, M., Bereiter, B., Blunier, T., Barnola, J.-M., Siegenthaler, U., Raynaud, D., Jouzel, J., Fischer, H., Kawamura, K., Stocker, T.F., 2008. High-resolution carbon dioxide concentration record 650,000–800,000 years before present. Nature 453, 379–382.

Martin, H.A., 2006. Cenozoic climatic change and the development of the arid vegetation in Australia. Journal of Arid Environments 66, 533–563.

Melillo, J.M., Aber, J.D., Linkins, A.E., Ricca, A., Fry, B., Nadelhoffer, K.J., 1989. Carbon and nitrogen dynamics along the decay continuum: plant litter to soil organic matter. Plant and Soil 115, 189–198.

Ning, Y.F., Liu, W.G., An, Z.S., 2008. A 130-ka reconstruction of precipitation on the Chinese Loess Plateau from organic carbon isotopes. Palaeogeography, Palaeoclimatology, Palaeoecology 270, 59–63.

O'Leary, M.H., 1988. Carbon isotopes in photosynthesis. Bioscience 38, 328–336.

Pagani, M., Freeman, K.H., Arthur, M.A., 1999. Late Miocene atmospheric CO_2 concentrations and the expansion of C_4 grasses. Science 285, 876–879.

Passey, B.H., Ayliffe, L.K., Kaakinen, A., Zhang, Z.Q., Eronen, J.T., Zhu, Y.M., Zhou, L.P., Cerling, T.E., Fortelius, M., 2009. Strengthened East Asian summer monsoons during a period of high-latitude warmth? Isotopic evidence from Mio-Pliocene fossil mammals and soil carbonates from northern China. Earth and Planetary Science Letters 277, 443–452.

Pearcy, R.W., Ehleringer, J., 1984. Comparative ecophysiology of C_3 and C_4 plants. Plant, Cell and Environment 7, 1–13.

Qiang, X.K., An, Z.S., Song, Y.G., Chang, H., Sun, Y.B., Liu, W.G., Ao, H., Dong, J.B., Fu, C.F., Wu, F., Lu, F.Y., Cai, Y.J., Zhou, W.J., Cao, J.J., Xu, X.W., Ai, L., 2011. New aeolian red clay sequence on the western Chinese Loess Plateau linked to onset of Asian desertification about 25 Ma ago. Science in China 54, 136–144.

Quade, J., Cerling, T.E., Bowman, J.R., 1989. Development of Asian monsoon revealed by marked ecological shift during the latest Miocene in northern Pakistan. Nature 342, 163–166.

Raven, P.H., Event, R.F., Eichhorn, S.E., 1999. Biology of Plants, sixth ed. W.H. Freeman and Company Worth Publishers, New York, 944 pp.

Shackleton, N.J., Crowhurst, S., Hagelberg, T., Pisias, N., Schneider, D.A., 1995a. A new late Neogene timescale: application to leg 138 sites. Proceedings of ODP, Scientific Results 138, 73–101.

Shackleton, N.J., Hall, M.A., Pate, D., 1995b. Pliocene stable isotope stratigraphy of ODP site 846. Proceedings of ODP, Scientific Results 138, 337–353.

Shackleton, N.J., Berger, A., Peltier, W.R., 1990. An alternative astronomical calibration of the Lower Pleistocene timescale based on ODP Site 677. Transactions of the Royal Society of Edinburgh: Earth Sciences 81, 251–261.

Shackleton, N.J., Pisias, N.G., 1985. Atmospheric carbon dioxide, orbital forcing, and climate. Geophysical Monograph Series 32, 412–417.

Sun, J.M., 2005. Long-term fluvial archives in the Fen Wei Graben, central China, and their bearing on the tectonic history of the India-Asia collision system during the Quaternary. Quaternary Science Reviews 24, 1279–1286.

Sun, J.M., Yie, J., Wu, W.Y., Ni, X.J., Bi, S.D., Zhang, Z.Q., Liu, W.M., Meng, J., 2010. Late Oligocene–Miocene mid-latitude aridification and wind patterns in the Asian interior. Geology 38, 515–518.

Sun, X.J., Song, C.Q., Wang, F.Y., Sun, M.L., 1995. Vegetations during the past 100,000-year on the Loess Plateau: pollen record of the Weinan loess section, Shanxi. Chinese Science Bulletin 43, 1222–1224 (in Chinese).

Sun, Y., Wang, X., Liu, Q., Clemens, S.C., 2010. Impacts of post-depositional processes on rapid monsoon signals recorded by the last glacial loess deposits of northern China. Earth and Planetary Science Letters 289, 171–179.

Vidic, N.J., Montañez, I.P., 2004. Climatically driven glacial–interglacial variations in C_3 and C_4 plant proportions on the Chinese Loess Plateau. Geology 32, 337–340.

Wang, H., Ambrose, S.H., Liu, C.J., Follmer, L.R., 1997. Paleosol stable isotope evidence for early Hominid occupation of East Asian temperate environments. Quaternary Research 48, 228–238.
Wen, Q.Z., 1989. Geochemistry of China Loess. Science Press, Beijing. 285pp., (in Chinese).
Yao, Z., Wu, H., Liang, M., Shi, X., 2011. Spatial and temporal variations in C_3 and C_4 plant abundance over the Chinese Loess Plateau since the last glacial maximum. Journal of Arid Environments 75, 881–889.
Zhang, Z., Zhao, M., Lu, H., Faiia, A.M., 2003. Lower temperature as the main cause of C4 plant declines during the glacial periods on the Chinese Loess Plateau. Earth and Planetary Science Letters 214, 467–481.
Zhao, J. (Ed.), 1995. China Geography, third ed. Advanced Education Press, Beijing, p. 342 (in Chinese).
Zhu, R.X., Laj, C., Mazaud, A., 1994. The Matuyama-Brunhes and upper Jaramillo transitions recorded in a loess section at Weinan, north-central China. Earth and Planetary Science Letters 125, 143–158.